PET Imaging Quantifying ^{68}Ga-PSMA-11 Uptake in Metastatic Colorectal Cancer

Tahleesa J. Cuda[1,2], Andrew D. Riddell[1,2], Cheng Liu[1,3,4], Vicki L. Whitehall[1,4], Jennifer Borowsky[1,2,4], David K. Wyld[1,2], Matthew E. Burge[1,2], Elizabeth Ahern[1,2,4], Alison Griffin[4], Nicholas J.R. Lyons[1,2], Stephen E. Rose[5], David A. Clark[1,2], Andrew R.L. Stevenson[1,2], John D. Hooper[1], Simon Puttick[5], and Paul A. Thomas[1,2,6]

[1]University of Queensland, Brisbane, Australia; [2]Metro North Hospital and Health Service, Brisbane, Australia; [3]Envoi Specialist Pathologists, Herston, Australia; [4]QIMR Berghofer Medical Research Institute, Herston, Australia; [5]CSIRO, Herston, Australia; and [6]Herston Imaging Research Facility, Herston, Australia

At diagnosis, 22% of colorectal cancer (CRC) patients have metastases, and 50% later develop metastasis. Peptide receptor radionuclide therapy (PRRT), such as ^{177}Lu-PSMA-617, is used to treat metastatic prostate cancer. ^{177}Lu-PSMA-617 targets prostate-specific membrane antigen (PSMA), a cell-surface protein enriched in prostate cancer and the neovasculature of other solid tumors, including CRC. We performed ^{68}Ga-PSMA-11 PET/CT imaging of 10 patients with metastatic CRC to assess metastasis avidity. Eight patients had lesions lacking avidity, and 2 had solitary metastases exhibiting very low avidity. Despite expression of PSMA in CRC neovasculature, none of the patients exhibited tumor avidity sufficient to be considered for ^{177}Lu-PSMA-617 PRRT.

Key Words: metastatic colorectal cancer; peptide receptor radionuclide therapy; PET; theranostics

J Nucl Med 2020; 61:1576–1579
DOI: 10.2967/jnumed.119.233312

Colorectal cancer (CRC) is the fourth most common cause of cancer-related death (*1*). At diagnosis, 22% of patients have metastases, and 50% develop metastasis during their lifetime (*1*).

Theranostics uses tumor-selective ligands conjugated to radionuclides and cytotoxic agents for, respectively, cancer imaging and treatment (*2*). By targeting tumor cell-surface antigens, these agents are delivered selectively to malignancies (*2*). Using a diagnostic positron-emitting radionuclide and PET, tumor burden is quantified and response to therapy predicted on the basis of tumor avidity (*2*). In peptide receptor radionuclide therapy (PRRT), therapeutic α- or β-emitting radionuclides, conjugated to the same PET imaging target, induce DNA damage and cell death (*2*). PRRT is a mainstay treatment for neuroendocrine tumors and is emerging for metastatic prostate cancer (PC) (*2*).

The PRRT target prostate-specific membrane antigen (PSMA) is enriched in metastatic PC and has low expression in normal tissues (*3,4*). It is also elevated on the endothelial cells of certain solid tumors, including CRC, where 75%–80% of primary tumors and metastases express PSMA, which correlates with poor outcome (*5,6*). PSMA-11, a high-specificity and high-affinity ligand for PSMA that incorporates a radiometal chelator (*7*), is applied for PET imaging of metastatic PC using ^{68}Ga-PSMA-11 (*8*) and PRRT using ^{177}Lu-PSMA-617 (*9*).

Several case reports note CRC avidity during ^{68}Ga-PSMA-11 imaging for metastatic PC, potentially supporting PSMA-targeted PRRT in advanced CRC (*10,11*). Responding to a recent call for prospective studies in place of incidental case reports or series (*12*), we assessed metastatic CRC avidity for ^{68}Ga-PSMA-11 to determine whether the avidity meets the criteria for ^{177}Lu-PSMA-617 PRRT.

MATERIALS AND METHODS

Patients

Inclusion and exclusion criteria (Supplemental Table 1; supplemental materials are available at http://jnm.snmjournals.org) and sample size ($n = 10$) were from PET imaging studies assessing tumor avidity (*8,13,14*). Recruitment would continue if initial results indicated that at least 30% of patients met the TheraP trial (NCT03392428) criteria to progress to PRRT.

PET Scans and Interpretation

The study had Human Research Ethics Committee approval (HREC/18/QPCH/51). Recruitment was from August to November 2018. Imaging used PSMA-11 (HBED-CC; ABX). ^{68}Ga was labeled as previously described (*15*), with a labeling efficiency of more than 98%. PET and CT images were reconstructed, and SUV_{max} and tumor-to-liver (background) SUV_{max} ratio were determined as previously described (*16*). ^{18}F-FDG PET/CT or contrast-enhanced CT localized metastases of low ^{68}Ga-PSMA-11 avidity, and SUV_{max} was compared between ^{68}Ga-PSMA-11 PET, ^{18}F-FDG PET, and contrast-enhanced CT. The TheraP trial criteria to stratify patients as likely responders to PRRT required an SUV_{max} of at least 10 at all tumor sites not subject to partial-volume artifact (i.e., >10 mm in diameter), an SUV_{max} of more than 20 at the most avid site, and ^{68}Ga-PSMA-11 avidity higher than ^{18}F-FDG avidity at all sites, when recent ^{18}F-FDG imaging was available (*17*).

Immunohistochemistry

The study had Human Research Ethics Committee approval (HREC/11/QRBW/453; P2139). Immunohistochemistry was performed on a tissue microarray of matched CRC primary tumors and metastases from 37 patients, using anti-PSMA clone 3E6 (Agilent) and Biocare Medical MACH1 mouse horseradish peroxidase polymer. Signal was quantified by a pathologist as nil, weak, moderate, or

Received Jul. 20, 2019; revision accepted Mar. 9, 2020.
For correspondence or reprints contact: Paul A. Thomas, Royal Brisbane and Women's Hospital, Butterfield St., Herston QLD 4029, Australia.
E-mail: paul.thomas@health.qld.gov.au
Published online May 1, 2020.

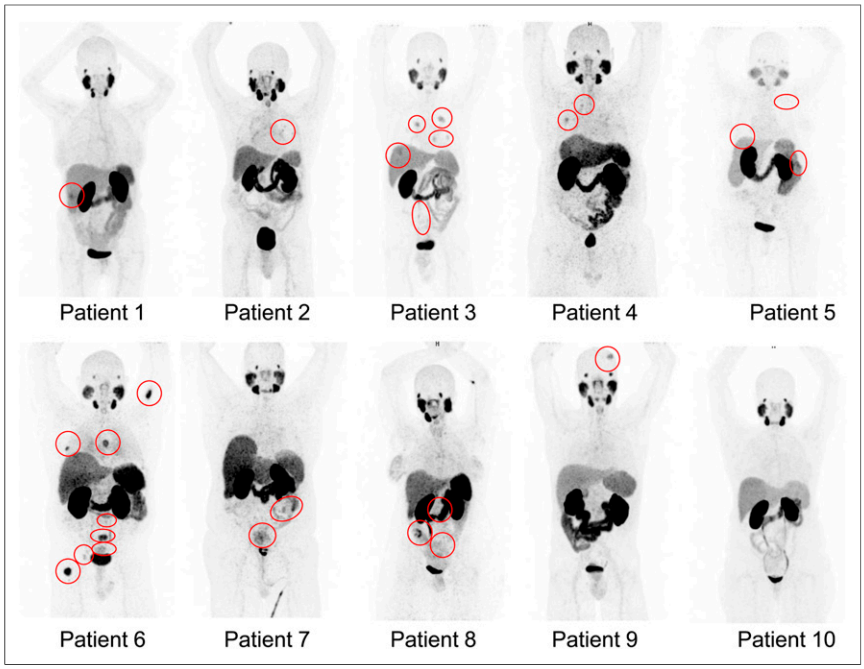

FIGURE 1. ^{68}Ga-PSMA-11 PET maximum-intensity-projection images of patients with metastatic CRC. Red circles = avid lesions.

strong on the basis of, respectively, no, ≤2.5%, ≥2.5–≤4.5%, or ≥4.5% positive tumor cells.

Statistical Methods

Statistics were performed using Prism (version 7; GraphPad). Data represent the highest SUV_{max} of representative lesions per anatomic region. Quantification was consistent with the reporting guidelines of the Standards for Reporting of Diagnostic Accuracy Studies (*18*).

RESULTS

^{68}Ga-PSMA-11 PET imaging of 10 patients with metastatic CRC (Supplemental Tables 2 and 3) resulted in no adverse events. Maximum-intensity projections of participants are shown in Figure 1, and SUV_{max} is in Figure 2, including TheraP criteria 1 and 2 (*19*). The metastases of all patients fell significantly short of satisfying criteria 1 and 2, except for liver lesions in patient 3 and lymph nodes in patient 8. Liver metastases in patient 3 met criterion 1 but not criterion 2. Patient 3 had synchronous lung and omental metastases that had insufficient avidity to satisfy criteria 1 and 2. Primary tumor and pelvic lymph node metastases in patient 8 exhibited avidity greater than criterion 1 but not criterion 2. This patient also had locoregional lymph node metastases that failed to satisfy criteria 1 and 2. Two of 3 patients with primary tumors (patients 6 and 7) failed to satisfy both criterion 1 and criterion 2. Bone metastases in patient 6 had the greatest avidity of all lesions and satisfied criterion 1 but fell just short of satisfying criterion 2. Locoregional and retroperitoneal lymph nodes and adrenal metastases in patient 6 failed to satisfy both criterion 1 and criterion 2.

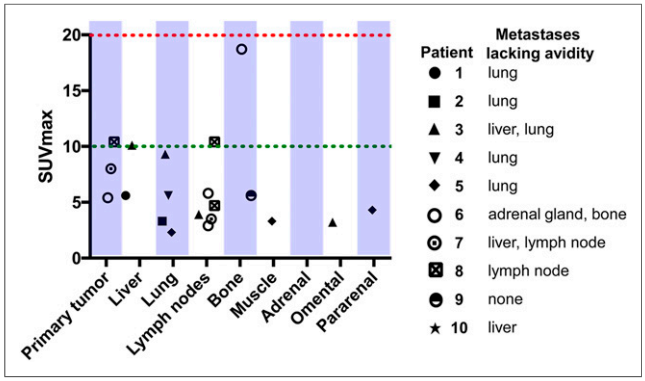

FIGURE 2. SUV_{max} of ^{68}Ga-PSMA-11 metastatic CRCs. Green line = TheraP criterion 1, $SUV_{max} \geq 10$, required at all sites. Red line = criterion 2, $SUV_{max} > 20$, required at most avid site.

Also of note, patient metastases lacked consistency in tumor-to-liver SUV_{max} ratios (Fig. 3) and no patient satisfied criterion 3 that ^{68}Ga-PSMA-11 avidity be greater than ^{18}F-FDG avidity (Supplemental Table 4). Supplemental Table 5 lists the lesions of each patient as detected by ^{18}F-FDG PET, contrast-enhanced CT, and ^{68}Ga-PSMA-11 PET, including the number missed by ^{68}Ga-PSMA-11 PET. The time between ^{68}Ga-PSMA-11 PET imaging and ^{18}F-FDG PET or contrast-enhanced CT is provided in Supplemental Table 6. Eight of 10 patients (patients 2, 3, 4, 5, 6, 7, 8, and 10) had lesions detected by ^{18}F-FDG PET or contrast-enhanced CT but missed by ^{68}Ga-PSMA-11 PET. Liver and lymph node metastases in patients 1 and 8 had heterogeneous uptake, with only a portion of lesions avid. Although patient 6 had bone metastases with significantly higher avidity during ^{68}Ga-PSMA-11 PET than other soft-tissue and visceral lesions, avidity was still significantly lower than ^{18}F-FDG PET avidity. Supplemental Figure 1 provides representative images of pelvic lymph node metastases with negligible avidity during ^{68}Ga-PSMA-11 PET, compared with high ^{18}F-FDG avidity, for patients 7 and 8. No lesions were detected by ^{68}Ga-PSMA-11 PET that were not also identified during ^{18}F-FDG PET. Patients 2, 3, 4, 9, and 10 had previously received neoadjuvant, adjuvant, or palliative chemotherapy, with patient 3 receiving palliative chemotherapy 8 weeks before ^{68}Ga-PSMA-11 PET, which likely had minimal effect on avidity because tumor response was poor. For the remaining 4 patients, at least 7 months had elapsed since chemotherapy.

Because resected tumors from the 10 patients were unavailable to explore the reason for the lack of tumor avidity, we performed immunohistochemistry for PSMA in matched primary tumors and metastases from an independent cohort of 37 patients (Supplemental Tables 7 and 8). PSMA was exclusive to endothelial cells of the tumor vasculature, which consistently comprised about 5% of the cells in tumors. Representative images of tumor regions displaying moderate (≥2.5–≤ 4.5% positive cells) and strong (≥4.5% positive cells) PSMA expression (Supplemental Fig. 2A) demonstrate that tumor expression was consistently very low. Quantitative analyses indicated that the invasive edge of 79% of primary tumors and 87% of central regions of primary tumors had nil or weak PSMA expression (Supplemental Figure 2B), with levels consistent between tumor regions (Supplemental

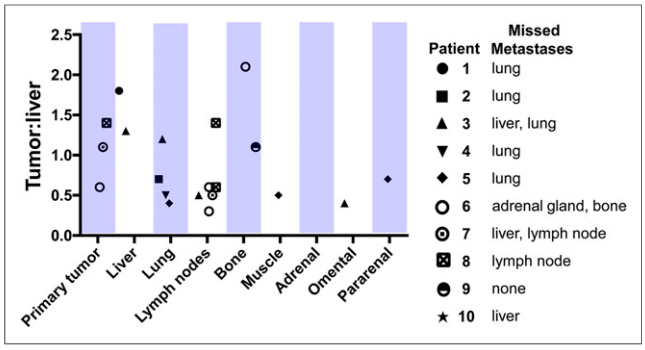

FIGURE 3. CRC tumor-to-liver (background) SUV_{max}.

Fig. 2C). In metastases, the invasive edge of tumors and the central region of 95% of tumors displayed nil or weak PSMA expression (Supplemental Fig. 2D), and expression was also consistent between these regions of metastases (Supplemental Fig. 2E). These data suggest that the low observed PSMA ligand avidity was due to consistently low PSMA expression in CRC tumors.

DISCUSSION

Responding to the recent call for prospective trials to assess the utility of PSMA-targeted theranostic agents for cancers beyond PC (*12*), this study indicated that ^{68}Ga-PSMA-11 PET has low avidity in metastatic CRC, with heterogeneous or nonexistent uptake in lesions. A range of factors may contribute to low tumor avidity, the most likely of which is low PSMA expression on tumor vasculature. Although PSMA expression has been reported on colorectal neovasculature (*5,6*), PSMA messenger RNA is 10–20 times lower in CRC than in PC (*19*), with our immunohistochemistry confirming low PSMA protein levels in CRC vasculature.

Although it is also possible that low avidity was due to a lack of homing of ^{68}Ga-PSMA-11 to CRC tumors, this is unlikely because we used a protocol that identifies metastatic PC and allows sufficient time for radioligand circulation, antigen binding, and internalization by PSMA-expressing cells (*8*). Other potential contributing factors include heterogeneous neovascularization and microvessel density in CRC lesions (*20*), tumor coopting of normal vessels lacking PSMA expression (*21*), and vascular mimicry with tumor blood-conducting channels lined by malignant cells (*22*).

We estimated that ^{68}Ga-PSMA-11 PET for metastatic CRC can be beneficial if tumor avidity is sufficient to progress at least 30% of patients to PRRT. However, none of the patients had sufficient avidity to progress to PRRT. Because our sample size was small, we cannot be definitive that ^{68}Ga-PSMA-11 PET is not justified for CRC. However, we note that, using binomial probability, there was only a very small chance (3%) that none of the 10 patients would have sufficient tumor avidity to warrant PRRT, justifying our decision not to continue recruitment beyond 10 patients.

CONCLUSION

^{68}Ga-PSMA-11 PET/CT is not sufficiently sensitive to detect metastatic CRC. Further research is required to identify cell-surface receptors as theranostic targets for imaging and treatment of CRC metastasis.

DISCLOSURE

The study was supported by the Redcliffe Private Practice Fund, the Royal Brisbane and Women's Hospital Foundation, and the Mater Foundation. No other potential conflict of interest relevant to this article was reported.

ACKNOWLEDGMENTS

We acknowledge the generous support of the Royal Brisbane and Women's Hospital radiochemistry staff in performing radiolabeling, the Herston Imaging Research Facility in performing PET/CT imaging, and the Royal Brisbane and Women's Hospital and the Redcliffe Hospital in recruiting patients.

KEY POINTS

QUESTION: Can PSMA expression on CRC neovasculature be targeted using ^{68}Ga-PSMA-11 with high sensitivity and avidity to qualify patients for ^{177}Lu-PSMA-617 therapy?

PERTINENT FINDINGS: This prospective pilot study assessed the tumor avidity of 10 patients with metastatic CRC using ^{68}Ga-PSMA-11. Overall, ^{68}Ga-PSMA-11 was insensitive in detecting CRC metastases. Identified lesions had avidity that was insufficient to warrant PSMA-targeted therapy.

IMPLICATIONS FOR PATIENT CARE: Theranostic ligands targeting specific receptors on metastatic CRC cells should be sought in place of targeting PSMA expressed by tumor neovasculature.

REFERENCES

1. Arnold M, Sierra MS, Laversanne M, Soerjomataram I, Jemal A, Bray F. Global patterns and trends in colorectal cancer incidence and mortality. *Gut.* 2017;66:683–691.
2. Turner JH. An introduction to the clinical practice of theranostics in oncology. *Br J Radiol.* 2018;91:20180440.
3. Tse BW, Cowin GJ, Soekmadji C, et al. PSMA-targeting iron oxide magnetic nanoparticles enhance MRI of preclinical prostate cancer. *Nanomedicine (Lond).* 2015;10:375–386.
4. Kiess AP, Banerjee SR, Mease RC, et al. Prostate-specific membrane antigen as a target for cancer imaging and therapy. *Q J Nucl Med Mol Imaging.* 2015;59:241–268.
5. Abdel-Hadi M, Ismail Y, Younis L. Prostate-specific membrane antigen (PSMA) immunoexpression in the neovasculature of colorectal carcinoma in Egyptian patients. *Pathol Res Pract.* 2014;210:759–763.
6. Haffner MC, Kronberger IE, Ross JS, et al. Prostate-specific membrane antigen expression in the neovasculature of gastric and colorectal cancers. *Hum Pathol.* 2009;40:1754–1761.
7. Benešová M, Schafer M, Bauder-Wust U, et al. Preclinical evaluation of a tailor-made DOTA-conjugated PSMA inhibitor with optimized linker moiety for imaging and endoradiotherapy of prostate cancer. *J Nucl Med.* 2015;56:914–920.
8. Hofman MS, Murphy DG, Williams SG, et al. A prospective randomized multicentre study of the impact of gallium-68 prostate-specific membrane antigen (PSMA) PET/CT imaging for staging high-risk prostate cancer prior to curative-intent surgery or radiotherapy (proPSMA study): clinical trial protocol. *BJU Int.* 2018;122:783–793.
9. Hofman MS, Violet J, Hicks RJ, et al. ^{177}Lu-PSMA-617 radionuclide treatment in patients with metastatic castration-resistant prostate cancer (LuPSMA trial): a single-centre, single-arm, phase 2 study. *Lancet Oncol.* 2018;19:825–833.
10. Huang YT, Fong W, Thomas P. Rectal carcinoma on ^{68}Ga-PSMA PET/CT. *Clin Nucl Med.* 2016;41:e167–e168.
11. Hangaard L, Jochumsen MR, Vendelbo MH, Bouchelouche K. Metastases from colorectal cancer avid on ^{68}Ga-PSMA PET/CT. *Clin Nucl Med.* 2017;42:532–533.

12. Salas Fragomeni RA, Amir T, Sheikhbahaei S, et al. Imaging of nonprostate cancers using PSMA-targeted radiotracers: rationale, current state of the field, and a call to arms. *J Nucl Med.* 2018;59:871–877.
13. Minamimoto R, Hancock S, Schneider B, et al. Pilot comparison of ^{68}Ga-RM2 PET and ^{68}Ga-PSMA-11 PET in patients with biochemically recurrent prostate cancer. *J Nucl Med.* 2016;57:557–562.
14. Sawicki LM, Buchbender C, Boos J, et al. Diagnostic potential of PET/CT using a ^{68}Ga-labelled prostate-specific membrane antigen ligand in whole-body staging of renal cell carcinoma: initial experience. *Eur J Nucl Med Mol Imaging.* 2017; 44:102–107.
15. Eder M, Lohr T, Bauder-Wust U, et al. Pharmacokinetic properties of peptidic radiopharmaceuticals: reduced uptake of $(EH)_3$-conjugates in important organs. *J Nucl Med.* 2013;54:1327–1330.
16. Rhee H, Blazak J, Tham CM, et al. Pilot study: use of gallium-68 PSMA PET for detection of metastatic lesions in patients with renal tumor. *EJNMMI Res.* 2016; 6:76.
17. Hofman MS, Emmett L, Violet J, et al. TheraP: a randomized phase 2 trial of ^{177}Lu-PSMA-617 theranostic treatment vs cabazitaxel in progressive metastatic castration-resistant prostate cancer (Clinical Trial Protocol ANZUP 1603). *BJU Int.* 2019;124(suppl 1):5–13.
18. Cohen JF, Korevaar DA, Altman DG, et al. STARD 2015 guidelines for reporting diagnostic accuracy studies: explanation and elaboration. *BMJ Open.* 2016;6: e012799.
19. Weinstein JN, Collisson EA, Mills GB, et al. The Cancer Genome Atlas Pan-Cancer analysis project. *Nat Genet.* 2013;45:1113–1120.
20. Kwak Y, Lee HE, Kim WH, Kim DW, Kang SB, Lee HS. The clinical implication of cancer-associated microvasculature and fibroblast in advanced colorectal cancer patients with synchronous or metachronous metastases. *PLoS One.* 2014; 9:e91811.
21. Qian CN, Tan MH, Yang JP, Cao Y. Revisiting tumor angiogenesis: vessel co-option, vessel remodeling, and cancer cell-derived vasculature formation. *Chin J Cancer.* 2016;35:10.
22. Baeten CI, Hillen F, Pauwels P, de Bruine AP, Baeten CG. Prognostic role of vasculogenic mimicry in colorectal cancer. *Dis Colon Rectum.* 2009;52:2028–2035.